JOURNAL OF MATERIALS SCIENCE 26 (1991) 4787–4794

Thermal analysis of hydrogenated amorphous carbon films prepared by plasma enhanced chemical vapour deposition

M. H. KIM, J. Y. LEE
Department of Materials Science and Engineering, Korea Advanced Institute of Science and Technology, Cheongryang P.O. Box 131, Seoul, Korea

Hydrogenated amorphous carbon (a–C:H) films were produced from propane and argon by an inductively coupled radio frequency (r.f.) glow discharge process under a particular deposition condition.

Thermal analysis for the deposit by GC, DSC, DTA, and TG gave information for the structural changes upon heating. Most C–H vibration spectra disappeared by heating up to 600 °C. The gas desorption began above 300 °C and reached maxima above 650 °C with several peaks. The desorption reaction was endothermic. Up to 600 °C the desorbed gases was not the hydrogen.

The large weight change was observed without the thickness reduction. The weight change rate was maximum at 480 °C. Hydrocarbons are believed to desorb below 600 °C.

A hydrocarbon desorption model is suggested. Hydrocarbons are formed in the inner surface of a microvoid and effuse out through the interconnected microvoids in the column boundaries. The proposed desorption reaction is also endothermic.

1. Introduction

Thin carbon films were produced by ionizing a hydrocarbon compound at relatively low temperature and moderately low pressure [1–7]. Utilization of these films for various applications has promoted researches into this field during recent years [8–15]. The film properties are directly related to the structural details of the film [1–15]. The variety that can be produced by varying the deposition conditions is infinite. Their structures were reported as graphitic, polymeric or diamond-like. The carbon films were generally described as diamond-like, i-carbon, and a-carbon films [16].

The hydrogens bonded in carbon films are important for the achievement of the desired properties for applications. The film microstructure also affects the properties. The gas desorption from a–C:H by heating has been investigated by several researchers to yield information on the bond state of hydrogen, the desorption mechanism, and the film microstructure [17–22]. They observed the disappearance of C–H vibration spectra with increasing annealing temperature by infrared (IR) spectroscopy. They considered the hydrogen as the desorption species, however the hydrogen is not still confirmed as the desorption species for all deposits.

Craig and Harding [17] observed the large quantities of H_2 and CO evolved from an a–C:H. Wild and Koidl [22] showed that hydrogen and/or hydrocarbons were effused from the deposits, however, they only discussed the gas desorption process by hydrogen. They did not explain the hydrocarbon desorption which would be important for some films obtained under particular deposition conditions.

This paper is concerned with the desorption behaviour of an a–C:H film during heat treatment. Thermal analysis is helpful to investigate the structural changes.

2. Experimental procedure

a–C:H films were produced by plasma enhanced chemical vapour deposition (PECVD) method in an inductively coupled glow discharge tube. A schematic diagram of the apparatus is presented in Fig. 1. The mixtures of propane and argon were introduced into the reactor. The vacuum chamber was a glass tube 65 mm in diameter and 700 mm in length. 13.56 MHz r.f. power with 50 Ω output is inductively coupled through an impedance matching to the reactor. The working coil was made of five turns of 6.4 mm diameter copper tube. A stainless steel tube was inserted to support the substrate holder. A thermocouple was inserted into the tube to measure the temperature of the substrate holder. The reactor was evacuated by a rotary mechanical pump. The pressure was measured by a U-manometer.

The typical deposition conditions presented in Table I, were selected to obtain high deposition rate of about 10 $\mu m\,h^{-1}$. Stable and local plasma were around the substrate surface. a–C:H was deposited onto both a polished silicon substrate and the stainless

0022–2461/91 $03.00 + .12

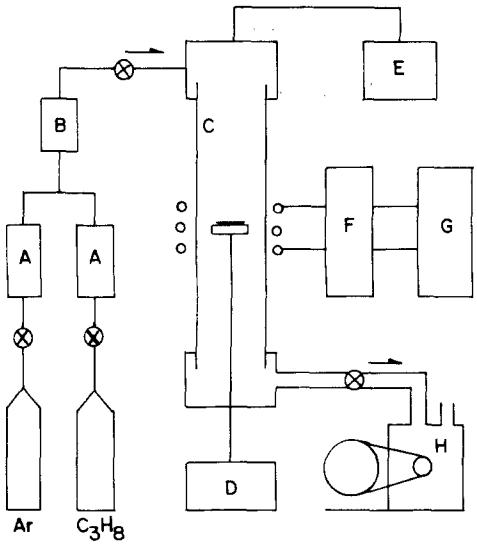

Figure 1 A schematic diagram of an inductive type radio frequency plasma enhanced chemical vapour deposition apparatus. (A flow meter, B gas mixer, C pyrex tube, D thermometer, E manometer, F impedance match, G rf generator, H rotary pump).

steel holder. At the end of a run the coating was cooled in argon atmosphere.

The film surface and the fractured cross-section were observed by SEM. The molecular bond structure was investigated by both conventional IR spectroscopy and Fourier transform infrared (FTIR) spectroscopy. The crystallinity of the deposit was checked by X-ray diffraction.

Thermal analysis by gas chromatography (GC), differential scanning calorimetry (DSC), differential thermal analyser (DTA), and thermogravimetry (TG) were conducted under a high purity argon (99.999%) atmosphere. Upon heating the desorption rate and the retention time of the desorbed gases were continually measured by GC. The evolution rates are defined by the amount of gas effused from the sample at regular time intervals. The retention time is the time for the effused gas flowing from the sample to the gas sensor in GC. The heat of reactions and the weight change were measured by using a Perkin-Elmer DSC-4 and a Rigaku TG-DTA.

TABLE I Typical deposition conditions for a–C:H films.

Deposition parameters	Range
total pressure (torr)	7–10
argon flow rate (sccm)	190
propane flow rate (sccm)	10
input r.f. power (W)	500
substrate temperature (°C)	400 ± 20
Deposition rate (μm h^{-1})	8–10
substrate holder – electrically grounded	

3. Results and discussion

3.1. Microstructure and bond state

Fig. 2a and b show SEM micrographs for the fractured cross-section and for the top view of a film deposited on a silicon substrate. The cross sectional morphology shows a change from smooth (less than 10 μm thickness) to close-packed columns with domed tops (Fig. 2b) with increasing thickness.

Fig. 3a and b show two surfaces with film thickness of 60 and 15 μm, respectively. The cracks are often found and the paths are always perpendicular to the substrate plane. The crack path of the thick film is rough due to large column sizes. X-ray diffraction did not take the form of any crystalline carbon even after heating up to 900 °C. The column boundaries are considered to be formed by the weakly bonded hydrogen clusters, which arise from the inhomogeneous hydrogen distribution. The film became brittle and porous, and was easy to crack after heat treatment.

The FTIR transmission of an as-deposited sample is shown in Fig. 4a. Fig. 4b is an enlarged spectra around 2900 cm^{-1}. Some absorptions are assigned in Table II. The strong bands around 2900 cm^{-1} suggest that the film contains lots of polymeric components [23]. The strong peak at 2925 cm^{-1} and, less strongly,

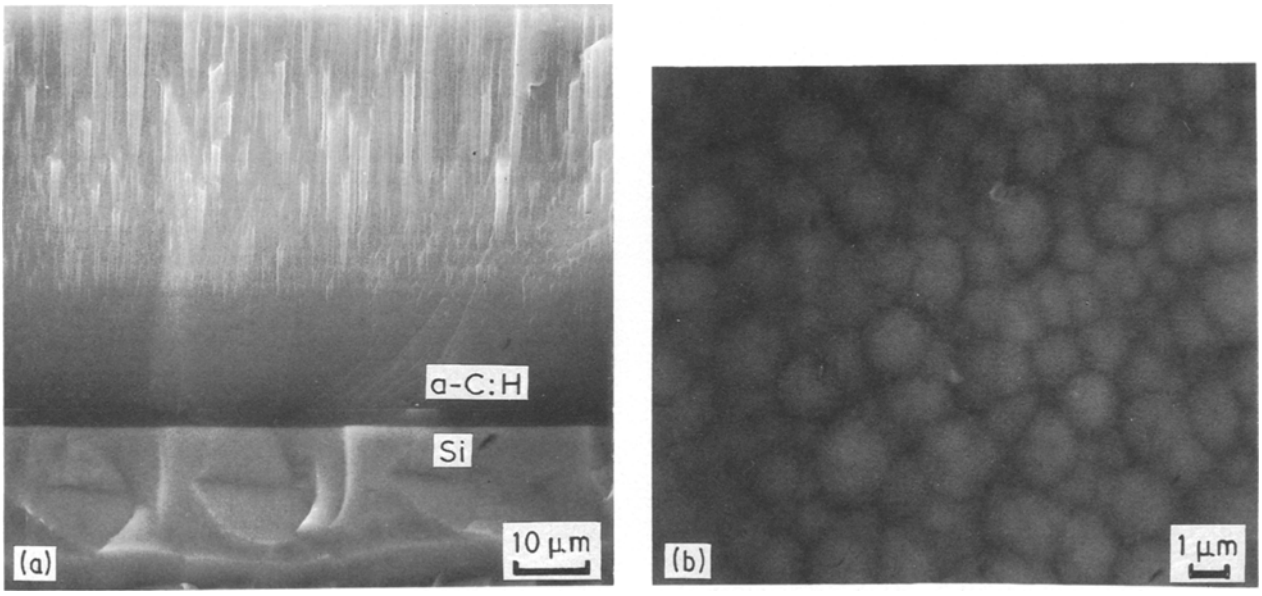

Figure 2 SEM micrographs (a) for the fractured cross-section and (b) for the top view of a film.

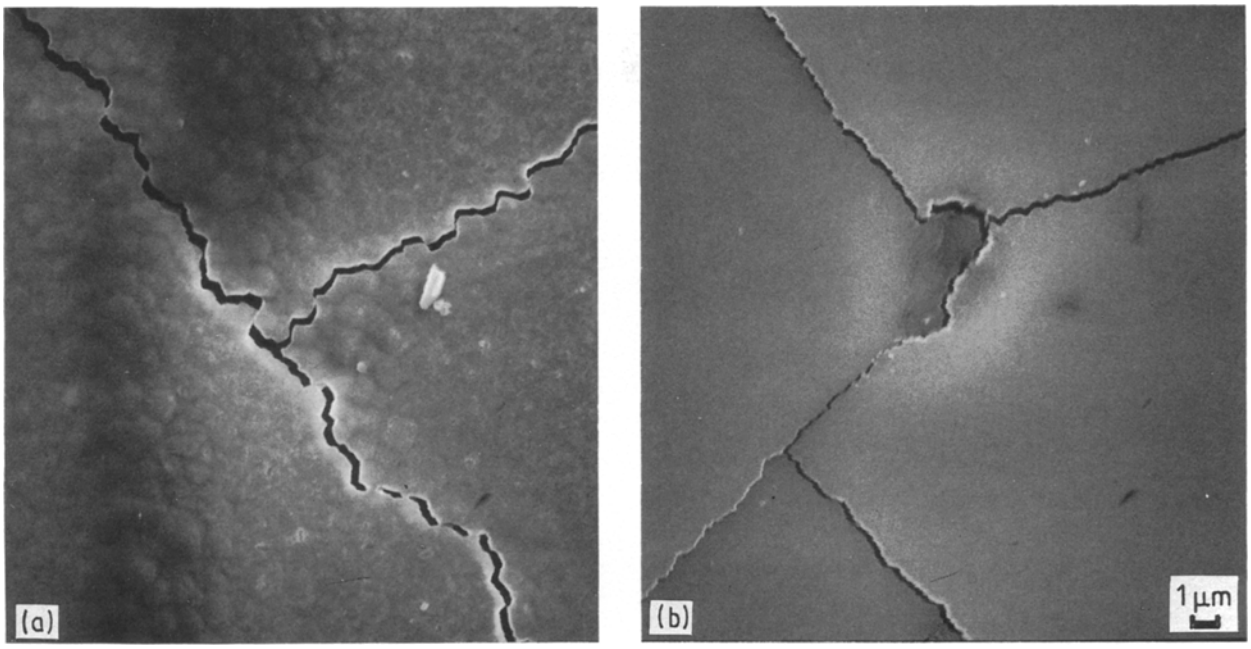

Figure 3 SEM micrographs for the top view of two deposits with thickness of (a) 60 μm and (b) 15 μm.

at 2850 cm^{-1} indicate that most hydrogens are tetrahedrally (SP^3) bonded to carbon. The tetrahedral dihydride (SP^3–CH_2) bond states are dominantly observed. The absorption peak at 1620 cm^{-1} indicates the carbon–carbon double bonds. Around 1400 cm^{-1}, (CH_n)C (n = 1, 2, or 3) type rocking vibration absorptions are found. The absorption by C=O stretch around 1700 cm^{-1} is relatively very weak. The network of a–C:H films are mixture of SP^3-type tetrahedral carbon bonds and SP^2-type threefold coordinated carbon bonds.

3.2. Gas desorption behaviour

Fig. 5 shows the change of IR spectra by heat treatments. C–H vibration modes almost disappeared at below 600 °C. Previous works by several researchers [17–21] proposed that the decrease of the absorption intensities arise from the desorption of the hydrogen. A recent investigation [22], however, showed that during heating to 600 °C the main desorption species were the hydrocarbons.

Fig. 6 shows the gas evolution behaviour of a deposit in argon atmosphere under constant heating rate of 3 °C min^{-1}. The evolution begins at about 300 °C and the evolution rate rapidly increases up to 650 °C. The onset point of the curve is near 400 °C.

Fig. 7 shows the change of retention time measured by GC. This is an appropriate parameter to differentiate the type of gases. Closed circles are for the desorbed gases from the deposit. Open circles are only for the hydrogen as a reference because a path of molecular-sieve is located between the sample and the gas sensor, the hydrogen takes a short time to pass through the sieve to the sensor. Larger molecules have longer retention times than hydrogen.

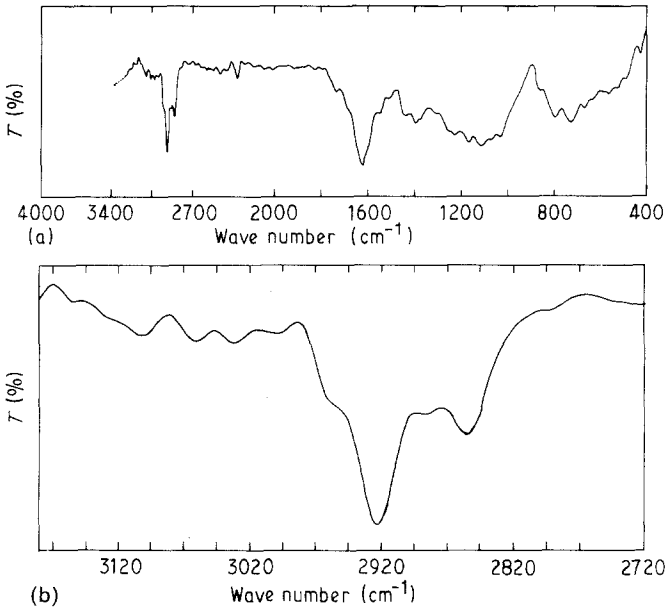

Figure 4 The FTIR transmission spectra of (a) an as-deposited sample and (b) an enlarged spectra around 2900 cm^{-1}.

TABLE II C–H stretch absorption bands, predicted and observed for a–C:H [18].

Configuration	Predicted frequency (cm^{-1})	Observed frequency (cm^{-1})	Relative intensity
SP^1CH (arom.)	3050	3060	very weak
SP^2CH_2 (olef.)	3020	3030	very weak
SP^2CH (olef.)	3000	2995	very weak
SP^3CH_3 (asym.)	2960	2960	medium
SP^2CH_2 (olef.)	2950	2950	weak
SP^3CH_2 (asym.)	2925	2922	very strong
SP^3CH	2915	2915	weak
SP^3CH_3 (sym.)	2870	2880	weak
SP^3CH_2 (sym.)	2855	2855	strong

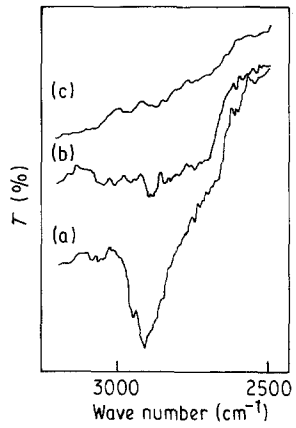

Figure 5 The change of conventional IR spectra of C–H stretch vibration by heat treatments. (a) an as-deposited sample, (b) after heating up to 550 °C, and (c) after heating up to 900 °C.

Below 600 °C the desorbed gases have longer retention times than hydrogen. The gases are not hydrogen. In recent study, Wild and Koidl [22] have presented some effusion spectra for a–C:H. They confirmed the hydrocarbons as main desorption species below 600 °C. Above 600 °C the desorbed gases were mainly hydrogen. The CO gas evolution discussed by Craig and Harding [17] is not considered here because of the very weak C=O absorption in Fig. 4a.

Fig. 8 is a DTA result for the deposit at a heating rate of 20 °C min^{-1} in argon atmosphere. The broken line is a reference curve of blank test. Above 300 °C the endothermic heat of reaction begins and the large peaks are at 480 and 550 °C. The strong endothermic peaks are at different temperatures with the gas evolution peaks.

The principle of the measurement by GC is thermal conduction of gases passing through the sensor. It is sensitive for the gas with high thermal conductivity. Hydrocarbon has lower capability for heat conduction than hydrogen, therefore below 600 °C the hydrocarbons are, not sensitively measured by GC but hydrocarbon desorption reaction is strongly endothermic.

Fig. 9 is a result of the thermogravimetric measurement accompanied by the DTA scan of Fig. 8. The weight loss increases with temperature and the rate (the slope of the curve) is maximum at 480 °C. This temperature coincides with the first endothermic peak in Fig. 8. The second endothermic reaction at 550 °C does not affect the curve in Fig. 9. An approximately 20% weight reduction suggests the desorption of hydrocarbon gases, because such a large weight loss is not explainable by hydrogen. Hydrocarbons are heavier than hydrogen. During heating the complex hydrocarbons are initially desorbed and followed by the light and simple hydrocarbon desorption.

If the main species are hydrocarbons below 600 °C, the desorption model must, therefore, be considered in terms of hydrocarbon formation and their related reactions.

a–C:H film was peeled from the silicon substrate by heating up to 800 °C in an argon atmosphere. Fig. 10a shows a SEM micrograph of the debris. Fig. 10b shows a cross-sectional view. The film surfaces became convex after the desorption of gases. The initial thickness was not, however, changed when compared with the as-deposited film.

The large weight loss exceeding 20% without a discernible thickness reduction is an important phenomenon. It gives information for the gas desorption model. If hydrocarbons are evolved after formation at

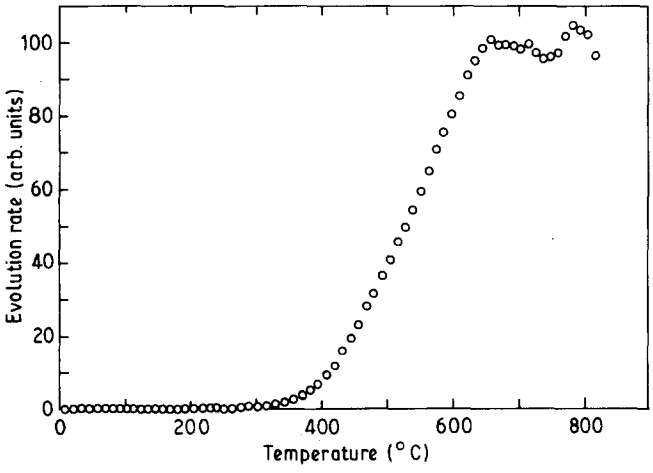

Figure 6 The gas evolution spectra from a deposit in argon atmosphere under a constant heating rate of 3 °C min^{-1} obtained by GC.

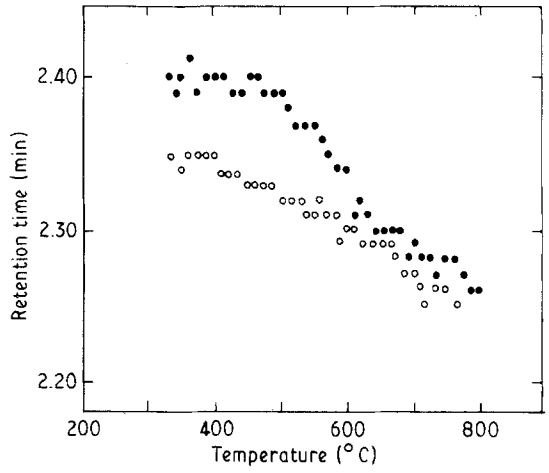

Figure 7 Plot of temperature against the retention times. Closed circles are for the desorbed gases from an a–C:H and open circles are for the reference hydrogen.

the film surface, the desorption process will result in a thickness reduction and will change the surface morphology to an irregular shape. The observed result, however, indicates that the hydrocarbons desorb from the inner region of the film.

The affect of oxidation is excluded as the surface oxidation will result in severe thickness reduction and will be largely exothermic.

The desorption reactions are also investigated by DSC. Fig. 11 represents five DSC curves for one sample under a constant heating rate of 3 °C min^{-1}. The heating and rapid cooling are sequentially repeated for the sample (curves 1 to 2). The endothermic reaction begins abruptly at the point B(1–5), which are the thresholds for the desorption reaction. Small peaks just over the step arise from the sample holder geometry. After heating up to C(1–4) the sample is then immediately quenched (−320 °C min^{-1}) to A(2–5). The thresholds for endothermic reactions (B2, B3, B4 and B5) coincide with the prior heating temperatures (C1, C2, C3, and C4), respectively.

Fig. 12 represents three DSC curves for one sample under a heating rate of 1 °C min^{-1}. Isothermal annealing affected the desorption reaction. The sample was isothermally annealed at C1 and C2 for 10 and 5 min respectively, and then quenched (− 320 °C min^{-1}), respectively. The threshold B2 and B3 of the second and third curve is 10 and 5 °C higher than C1 and C2. The thresholds shifted to high temperatures by the previous annealing time.

The carbon and hydrogen in amorphous structure are randomly bonded so that the bond energies are not the fixed values. The local atomic arrangement and the bond strengths affect the bond energies of various C–CH_n bonds. With increasing temperature the close neighbours of C–CH_n pairs interact to form hydrocarbons and desorb initially. Thereafter more distant pairs may interact each other. Hydrocarbons are formed by thermal activation process. The threshold shiftings by isothermal annealing (Fig. 12) are

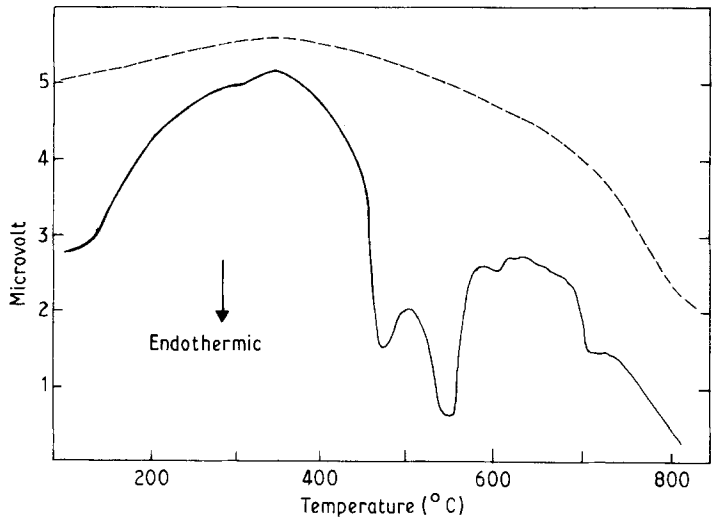

Figure 8 A DTA curve for the same deposit in Fig. 5 in argon atmosphere and under a heating rate of 20 °C min^{-1}. The broken line is a reference curve of a blank test.

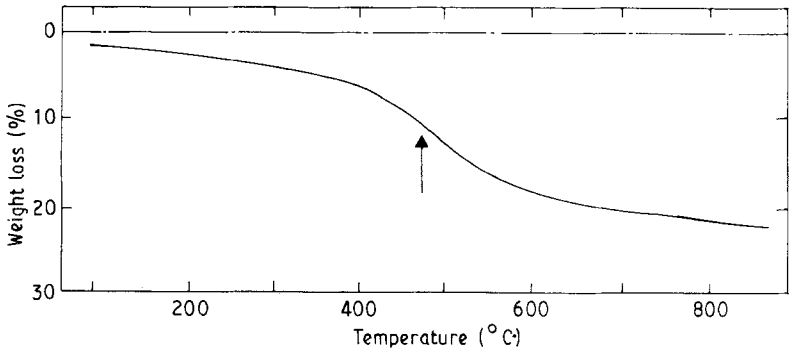

Figure 9 A TG curve accompanied with the DTA in Fig. 7. The initial sample weight was 11.5 mg.

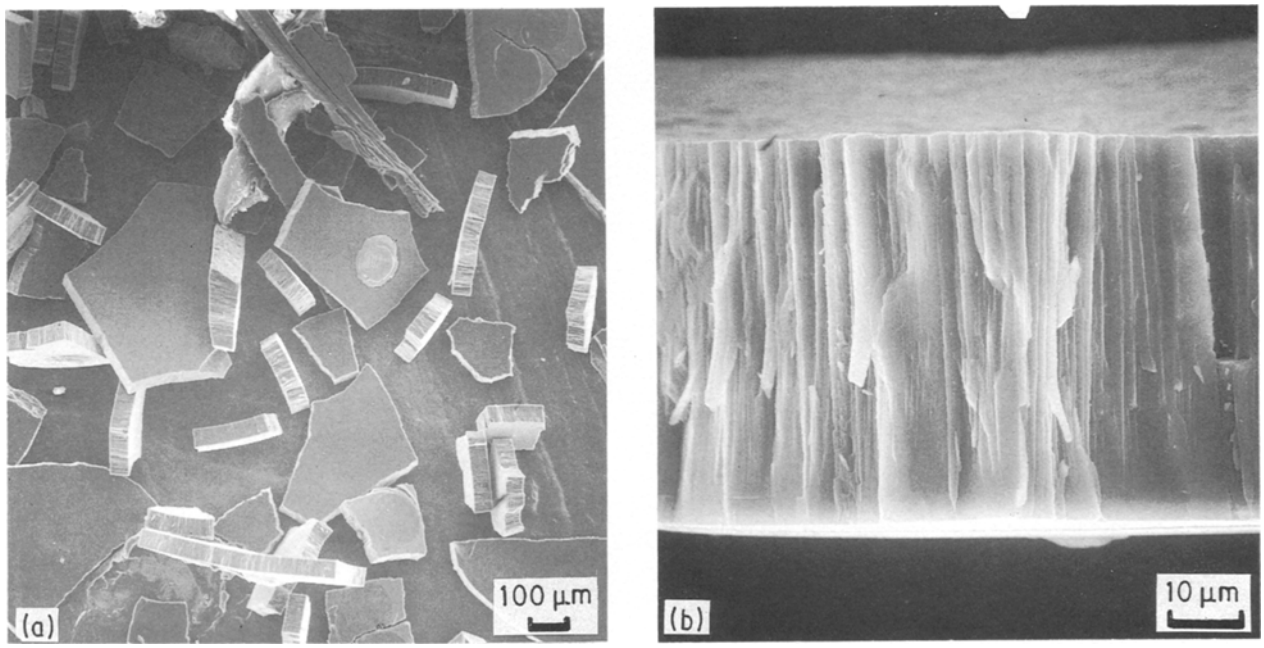

Figure 10 SEM micrographs of (a) debris peeled off from silicon substrate after heating up to 900 °C and (b) a cross-sectional view.

considered as the result of the increased thermal activation barrier.

3.3. A proposed desorption model

Fig. 13 shows a schematic diagram of a tetrahedral carbon network. The network is modified by dihydride (SP^3–CH_2) and trihydride (SP^3–CH_3) based on the infrared results in Fig. 4a. The network distortion is not considered here.

Table III represents the average energies for some types of bonds. Carbon–carbon single bond has the lowest one than others. Therefore the C–C single bond breaking is energetically more favourable than the breaking of C–H bond. This is very consistent with the desorption of hydrocarbons prior to the hydrogen.

One of the possible interactions is presented in Fig. 14. The considerable hydrocarbon desorption will increase the amount of dangling bonds. The reactions between the excess dangling bonds are exothermic. The interaction has several reaction steps. The reaction energies are simply calculated from Table III. They will have somewhat deviant bond energies due to the distortion in amorphous network.

TABLE III Average bond energies and bond lengths at 25 °C [17].

Type of bond	Average bond energy (eV)	Average bond length (nm)
C–C	3.6	0.154
C=C	6.4 (* = 2.8)	0.134
C–H	4.0	0.108
H–H	4.5	0.074

* indicates the increment in bond energy associated with the formation of an additional bond.

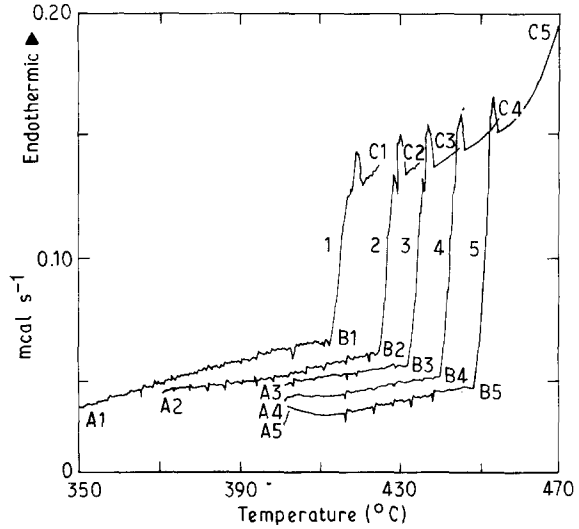

Figure 11 Five consecutive DSC curves for an a–C : H. The thresholds move to high temperatures by the previous heatings.

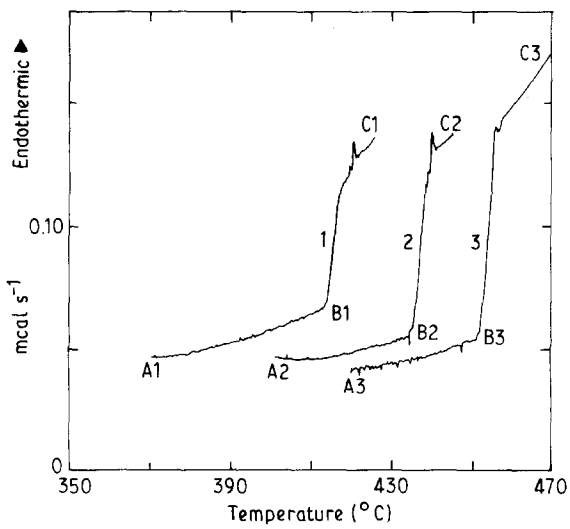

Figure 12 Three consecutive DSC curves for an a–C : H. The sample was annealed for 10 min and 5 min at C1 and C2, respectively.

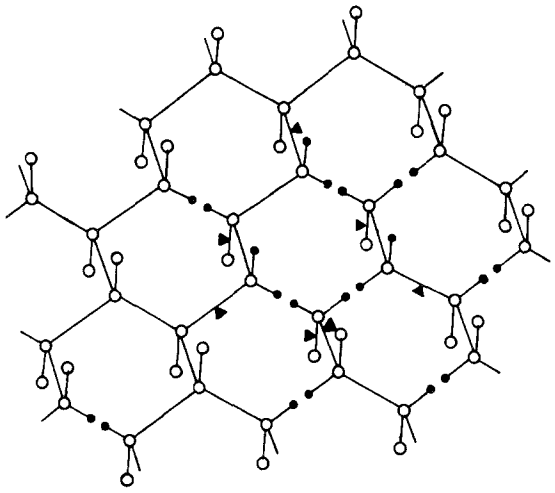

Figure 13 A schematic diagram of a randomly hydrogenated carbon network based on Fig. 4. (● hydrogen, ○ carbon, ▲ bond breaking)

The shape of the DTA curve is very dependent on the initial atomic arrangement. The reaction heat as endothermic or exothermic for hydrocarbon desorption can be determined by the relative dominance of the competing reactions. These are the bond breakings, the hydrocarbon formations, dangling bonds interaction, and the structural rearrangement.

It is believed that hydrocarbons are effused after creation in the internal surface of a microvoid. The path for the molecular transport of the hydrocarbons through the amorphous network is suggested. The column boundaries shown in Fig. 2a are considered to be one of the paths. An interconnected microvoid can be easily formed in the hydrogen clustered column boundary regions. Not only the hydrocarbon formation but also the path formation may also limit the hydrocarbon transport through the film.

Hydrogen is considered to desorb above 600 °C. The hydrogen effusion was discussed by Wild and Koidl [22]. Several researchers suggested the hydrogen desorption model [19–21].

We examined the sample of a particular deposition condition. For obtaining the sufficient deposits for analysis the deposition conditions was very restricted. Although the influence of the deposition parameters is not given here, the thermal analysis results are, at least, helpful to understand the structure of a–C:H. Further work to determine the affect of the deposition parameters on the desorption behaviour will be needed to understand the effusion mechanism more clearly.

4. Conclusions

The conclusions are as follows.

(1) a–C:H films were deposited under a particular deposition condition. The hydrogens were tetrahedrally bonded to carbon atoms. The microstructure changed from smooth to columnar with increasing film thickness.

(2) The structural changes upon heating were investigated by the thermal analysis by GC, DSC, and TG-DTA. The hydrocarbons desorbed below 600 °C as the endothermic reaction. The threshold for hydrocarbon desorption was increased to high temperature by the supplied thermal energy.

(3) A hydrocarbon desorption model was proposed. The hydrocarbons are formed in the inner surface of a microvoid. The effusion paths are the interconnected voids in the column boundaries.

(4) The thermal analysis technique is very useful to obtain the structural information. Continuous observations upon heating make it possible to understand the desorption reaction. Further work on the affect of deposition conditions will help to study the desorption mechanism more clearly.

References

1. L. P. ANDERSSON, *Thin Solid Films* **86** (1981) 193.
2. S. AISENBERG and R. CHABOT, *J. Appl. Phys.* **42** (1971) 2953.
3. L. HOLLAND and S. M. OHJA, *Thin Solid Films* **38** (1976) L17.
4. *Idem., ibid.* **58** (1979) 107.
5. D. A. ANDERSON, *Phil. Mag.* **35** (1977) 17.
6. R. MESSIER, A. R. BADZIAN, T. BADZIAN, K. E. SPEAR, P. BACHMANN, and R. ROY, *Thin Solid Films* **153** (1987) 1.
7. H. VORA and T. J. MORAVEC, *J. Appl. Phys.* **52** (1981) 6151.
8. H. TSAI and D. B. BOGY, *J. Vac. Sci. Technol.* **A5** (1987) 3287.
9. K. FABISIAK, S. ORZESZKO, F. ROZPLOCH, and J. SZATKOWSKI, *J. Non-Cryst. Solids* **99** (1988) 12.
10. V. J. KAPOOR, *J. Vac. Sci. Technol.* **A4** (1986) 1013.
11. R. MEMMING and H. J. TOLLE, *Thin Solid Films* **143** (1986) 31.

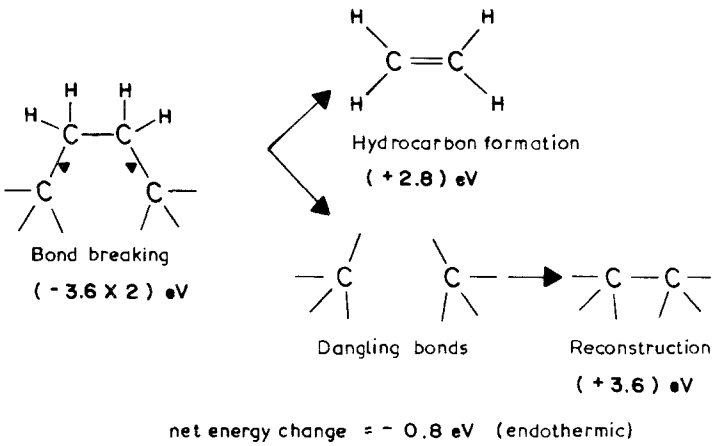

Figure 14 One of the possible interactions to form a hydrocarbon from Fig. 13.

12. S. F. PELLICORI, C. M. PETERSON, and T. P. HENSON, *J. Vac. Sci. Technol.* **A4** (1986) 2350.
13. F. W. SMITH, *J. Appl. Phys.* **55** (1984) 764.
14. D. R. McKENZIE, R. C. McPHEDRAN, N. SAVVIDES, and L. C. BOTTEN, *Phil. Mag. B* **48** (1983) 341.
15. N. SAVVIDES, *J. Appl. Phys.* **59** (1986) 4133.
16. J. C. ANGUS, *Thin Solid Films* **142** (1986) 145.
17. S. CRAIG and G. L. HARDING, *ibid.* **97** (1982) 345.
18. B. DISCHLER, A. BUBENZER, and P. KOIDL, *Solid State Commun.* **48** (1983) 105.
19. M. P. NADLER, T. M. DONOVAN, and A. K. GREEN, *Thin Solid Films* **116** (1984).
20. R. MEMMING, *ibid.* **143** (1986) 279.
21. P. COUDERC and Y. CATHERINE, *ibid.* **146** (1987) 93.
22. C. WILD and P. COIDL, *Appl. Phys. Lett.* **51** (1987) 1506.
23. L. J. BALLAMY, "The Infrared Spectra of Complex Molecules" (London, 1964).

Received 24 October 1989
and accepted 19 March 1990